

# The effect of mountain wind on the falling snow deposition

Zhengshi Wang<sup>1,2</sup> and Ning Huang<sup>1,2</sup>

<sup>1</sup>Key Laboratory of Mechanics on Disaster and Environment in Western China (Lanzhou University), the Ministry of Education of China, 730000

<sup>2</sup>Department of Mechanics, School of Civil Engineering and Mechanics, Lanzhou University, Lanzhou, 730000, China

Corresponding to: wangzhsh2013@lzu.edu.cn

**Abstract.** The air-flow over morphologic prominence is of vital importance for the temporal and spatial variations of snow distribution, which may further affect the hydrological cycle, climate system, ecological evolution as well as other natural processes. Most previous studies have neglected the effect of non-uniform mountain wind on the trajectory of falling snow particle and thus the uneven snow distribution over complex terrain is little known. Here in this paper, we carry out a numerical study on the deposition process of mixed grain size snow particles over mountain terrains. A three-dimensional large eddy simulation (LES) code is used to predict the wind field and the fluid-solid coupling effect is considered, the Lagrangian particle tracking method is employed to track the movement of each falling snow particle. Our results suggest the boundary layer flow over steep slopes or complex terrains exhibits obvious uneven characteristics. The mountain wind has obvious effect on the motion of snow particles and finally results in a non-uniform distribution of snow. This research is of significance to understand the evolution of high resolution snow distribution in cold highland areas.

## 1. Introduction

Snow is widely distributed on Earth with significant interannual and seasonal variations. Subject to the action of wind, snow always shows a nonuniform distribution especially in mountainous areas with complex terrain. On the one hand, the distribution unevenness in the mountainous areas may induce and aggravate snow floods, avalanche, mudslides, landslide and other natural disasters [1], which not only results in huge direct and indirect economic losses, but also may cause casualties. On the other hand, some characteristics of snow cover, such as the snow cover area, the snow distribution and snow depth, are important input parameters of global energy balance, climate, hydrological and ecological models. Thus, to understand the evolution of high resolution snow distribution is essential.

At this stage, snow distributions are mainly examined from field measurement or pattern prediction. For the observation, remote sensing retrieval is the most commonly used method, such as the multispectral imaging AVHRR (Advanced Very High Resolution Radiometer) [2] and moderate resolution spectral image MODIS (Moderate Resolution Imaging Spectroradiometer) [3, 4]. The temporal and spatial resolution of remote sensing retrieval is poor for snow cover changes fast along with snowfalls, and the accuracy of remote sensing retrieval could not cope due to the interference of various nature factors. In addition, almost all the inversion algorithms for the remote sensing have a strong geographical restriction [5]. For example, the AVHRR does not apply to the complex terrain. More importantly, the snow depth cannot be acquired by remote sensing retrieval. On the other hand, large amount of studies on the snow distribution over complex terrain have been conducted by many



researchers. Such as, the seeder-feeder mechanism [6-9] is described to be the main process to generate the enhancement of precipitation over terrains. And Houze [10] went on a study about the fundamental formation process of precipitation cloud for different terrains and conditions. On a much smaller scale that near the topography surface, the variation of advecting and vertical winds contributes greatly to the falling trajectories of snow grains and results in the locally enhanced deposition [8, 11-13]. However, most models or patterns pay little attention to the real motion processes of the falling snow particles. In other words, the behaviors of falling particles in the complex turbulent boundary layer on snow distribution are neglected.

In this paper, the Lagrangian particle tracking model was introduced into ARPS, and the interaction between particles and wind flow is taken into account. An imaginary snowstorm over rugged terrain is performed through tracking the trajectory of each falling snow particle. Then the snow deposition condition around the terrain is simulated. Finally, the movement feature of snow particles in the air and the distribution of snow on the ground are analyzed in detail.

## 2. Model and methods

### 2.1. Wind field prediction and particle motion

The Large Eddy Simulation (LES) method is used to simulate the wind field and the source code is obtained from ARPS. ARPS is developed by the University of Oklahoma that incorporates numerical simulation, data assimilation and data processing [14, 15].

The filtered three-dimensional, nonhydrostatic and fully compressible Navier-Stokes equations can be written as:

$$\frac{\partial \bar{\rho} \tilde{u}_i}{\partial t} + \frac{\partial \bar{\rho} u_i \tilde{u}_j}{\partial x_j} = -\frac{\partial \tilde{p}^*}{\partial x_i} - \frac{\partial \tau_{ij}}{\partial x_j} + B \delta_{i3} + F_i \quad (1)$$

where the tilde symbol indicates the filtered variables and line symbol represents grid volume-averaged variables.  $x_i$  ( $i=1,2,3$ ) indicate the coordinates of streamwise, spanwise, and vertical directions, respectively;  $u_i$  is the instantaneous velocity component,  $\bar{\rho}$  is the grid volume-averaged air density and  $t$  is time,  $\tau_{ij}$  is the subgrid stress tensor and  $\delta_{ij}$  is the Kronecker delta;  $p^* = p' - \alpha \nabla(\bar{\rho} \mathbf{u})$  is the logogram of the pressure deviations and a divergence damping terms designed to attenuate acoustic waves, in which the  $\Delta$  represents the divergence and  $\alpha$  is the damping coefficient.  $B = -g \rho' / \bar{\rho}$  is the buoyancy term comes from the density fluctuation  $\rho'$ ,  $g$  is the gravitational acceleration.

To take into consideration of the reaction force of snow particles in the air on the wind field, a volume force  $F_i$  is added in the right side of Equation (1), which can be written as [16]:

$$F_i = -N \frac{1}{\rho V_{grid}} \sum_{s=1}^{N_p} m_p \frac{u_i(x_p(t), t) - u_{pi}(t)}{T_p} f(Re_p) \quad (2)$$

in which,  $N_p$  and  $V_{grid}$  are respectively the particle number and the volume of the grid cell.  $m_p$  is the mass of snow particle,  $u_{pi}(t)$  and  $u_i(x_p(t), t)$  are the velocity of snow particle and the wind velocity at the location of grain at time  $t$ , respectively;  $T_p = \rho_p d_p^2 / 18 \rho \nu$  represents the particle response time and  $N$  means that one particle represents  $N$  snow particles for the purpose of reducing computation.

$f(Re_p)$  can be express as [17]:

$$\begin{aligned} f(Re_p) &= 1 & (Re_p < 1) \\ f(Re_p) &= 1 + 0.15 Re_p^{0.687} & (Re_p \geq 1) \end{aligned} \quad (3)$$

where  $Re_p = d_p |u - u_p| / \nu$  is the particle Reynolds number and  $\nu$  is the kinematic viscosity of air.

The snow particles are assumed to be only subject to gravity and drag force in the air, and the governing equation of particle motion can be expressed as [18-20]:

$$\frac{du_{pi}}{dt} = \frac{3\rho\nu(u_i - u_{pi})}{4\rho_p(d_p)^2} C_D Re_p + g_i \left(1 - \frac{\rho}{\rho_p}\right) \quad (4)$$

where  $C_D Re_p$  can obtain from Wallis' empirical formula:

$$C_D Re_p = \begin{cases} 24 + 3.6(Re_p)^{0.687}, & (Re_p \leq 1000) \\ 0.44 Re_p, & (Re_p > 1000) \end{cases} \quad (5)$$

## 2.2. Wind field prediction and particle motion

The study area is in the Qilian Mountains in northwestern China (E100°14'15", N38°00'50.4"), as shown in Fig. 1, and the topographic data for this study are derived from a DEM database with 30 m resolution. The initial base state wind is set as horizontally homogeneous logarithmic profile based on the field measurement. The atmosphere boundary layer is assumed to be stably stratified. The humid atmosphere is simulated with the constant relative humidity of 90% based on the measurement in the snowfall processes. The roughness length is 0.01 m and the boundary layer initial depth is set as 500m.

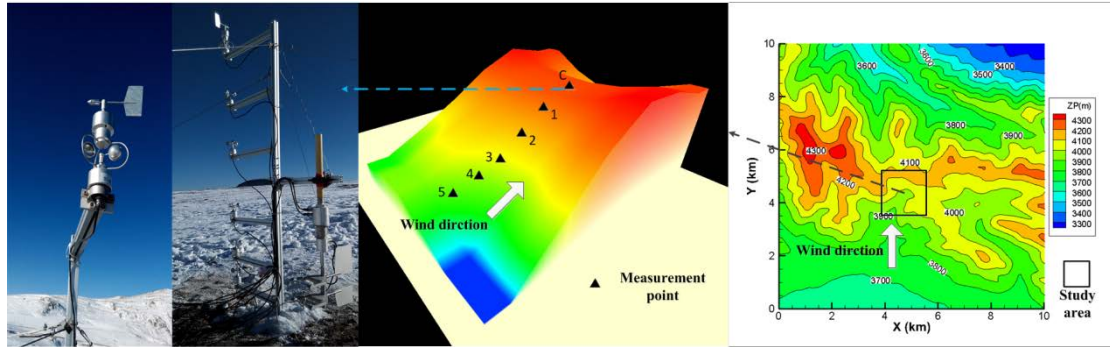


**Figure 1.** The study area and measurement point schematic diagram

The rigid ground boundary condition is applied at the ground and a Rayleigh damping layer is used at the top of the domain (1000 m in depth). Along the lateral boundaries, the open radiation boundary conditions are used. The snow particle size is gamma distributed and the periodic boundary conditions are used for the snow grains. The periodic boundary cannot be used in the flow field because the terrain is unsymmetrical, this may lead to slightly deviation near the boundary. In order to avoid this influence, a much bigger computational domain is selected. In our simulation, the dimensions of the computational domain are set at 10 km×10 km×4 km and the study area is 2 km×2 km×4 km. The grid has a uniform horizontal size of 50 m and the nested grid size is 5 m. In the vertical direction, the grid is stretched with a cubic function for the purpose of acquiring more detailed information on the surface layer. The mean vertical grid space is 50 m and the smallest grid is 2 m. This grid resolution is necessary to reproduce the small-scale flow features of complex terrains [21].

## 3. Result and discussion

The snow deposition around the terrain under the condition of uniform snowfall is simulated based on the coupled LES and particle tracking pattern. The total simulation time is 2 hours. First of all, the wind field without particle is analyzed. Figure 2 is the ground surface (2 m height) wind vector map of the study area at T=4200 s. As can be seen from the figure, the wind is accelerated significantly on the windward slope and there formed some clear recirculation zones and vortexes on the leeward slope. In addition, the flow around the topography is quite clear. To further analyze the wind speed information,

the wind speed-up ratio on the windward slope is calculated and the result is compared with the observation results, in which the speed-up ratio is a mean value of 60 seconds and equal to the specific value of local wind speed and reference wind speed at measurement point C. It can be seen that the simulated wind speed-up ratio is consistent with the experimental results. In this condition, the particle is introduced into the calculation. In our simulation, the snow particles fall uniformly from the height of 5000m (the reference ground height is 3000m) with a release rate of 10000 particles per second, and the initial velocity of each snow particle is zero.

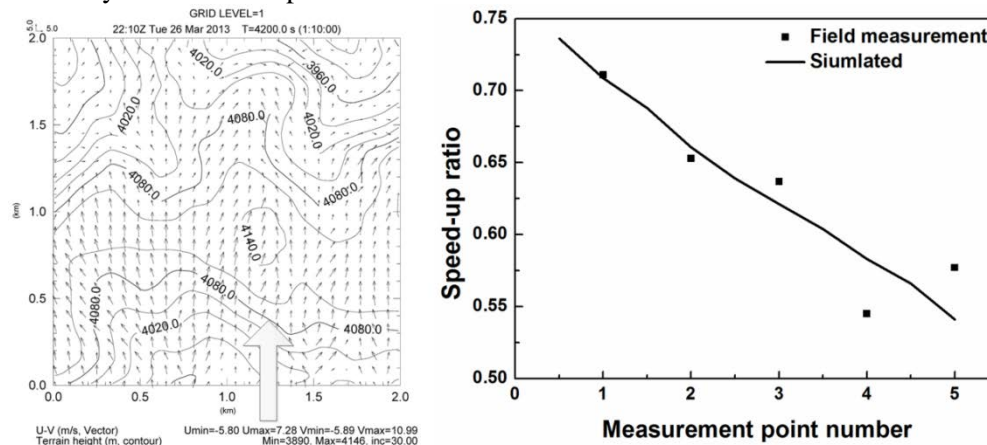


**Figure 2.** The wind vector illustration of study area and the wind speed-up ratio of the measurement point.

The probability distributions of one hour averaged vertical wind speed (10m in height) and the particle falling speed (into the boundary layer) are displayed in Figure 3, in which the positive values mean the up direction and the red lines represent that the coupling effect between particles and wind flow is included. It can be seen from this figure that the proportion of larger vertical wind speed increases when the coupling effect is considered. The percentage of absolute value of vertical wind speed increases from 19.2% to 32.7%. At the same time, the falling velocity of snow particles is obviously changed if the coupling effect is included. As shown in the figure, another peak value appeared with the coupling effect. The percentage of smaller terminal velocity is obviously increased because the increase of the upward-moving particles.

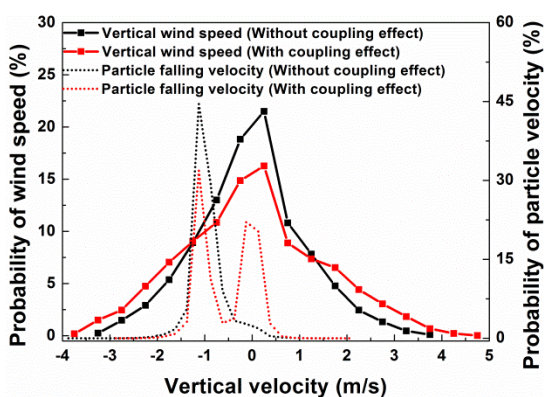


**Figure 3.** The probability distributions of vertical wind speed and particle falling velocity.

Figure 4 shows the evolution of snow depth distribution of the study area at different times. The circle on the map is at the windward slope position and the dotted circle represents the leeward slope position. We select 10 points in the circle to obtain the mean snow depth. As shown in the figure, there is significant difference in snow depth at different locations of complex terrains. In general, snow particles are easier to accumulate on the windward slope than on the leeward slope, and the difference between windward slope and leeward slope intends to become larger with time. For example, the average snow depth of windward slope (solid circle) and leeward slope (dotted circle) is almost equal

at  $t=30$  min. However, at  $t=60$  min and  $t=90$  min, the mean snow depth on the windward slope are respectively 0.545 mm and 0.987 mm, and the average snow depth on the leeward slope are 0.364 mm and 0.503 mm, respectively. The average snow depths of windward slope are 1.497 times and 1.962 times of leeward slope at  $t=60$  min and  $t=90$  min, respectively. This is mainly because the updraft on the windward slope has an inverse influence on the particle fall velocity and thus snow particles will convergence on the windward.

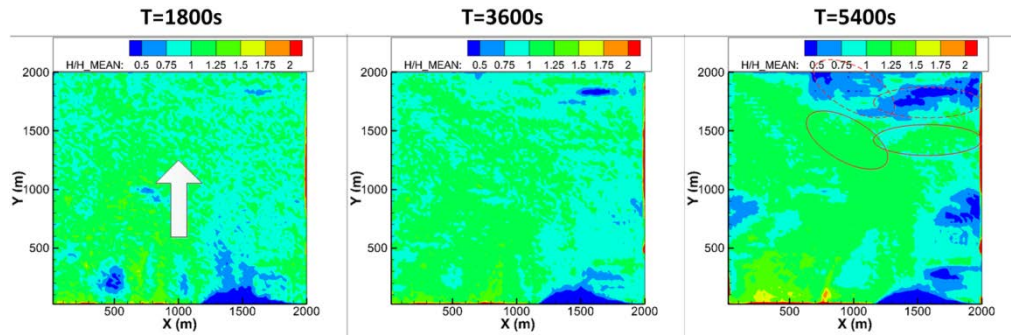


**Figure 4.** Snow deposition mass ( $\text{kg/m}^2$ ) of study area at different time.

#### 4. Conclusions

The Lagrangian particle tracking model is introduced into ARPS Numerical Simulation System and the snowfall deposition process over rugged terrain is simulated. The coupling effect between snow particles and air flow is considered. The snow deposition mass and velocity distributions are obtained through statistical method. The main conclusions are as follows:

- 1) The wind field is non-uniform over rugged terrain. The wind velocity and direction vary greatly at different positions. In general, the wind is accelerated in the windward slope; there are large amount of recirculation zones and vortexes in the leeward slope.
- 2) The updraft has obvious influence on the fall velocity of snow particles in the air. The percentage of smaller terminal velocity or even upward-moving particles is obviously increased under the action of updraft.
- 3) The non-uniform mountain wind is an important mechanism to enhance the uneven distribution of the orographic precipitation and snow particles are easier accumulated on the windward slope than on the leeward slope.

#### Acknowledgments

This work is supported by the Major projects of national forestry public welfare industry research (201404306).

#### References

- [1] Michaux J L, Naaïm-Bouvet F and Naaïm M 2001 Drifting-snow studies over an instrumented mountainous site: II. Measurements and numerical model at small scale *Annals of Glaciology* **32**(1) pp 175-81
- [2] Zheng Z J, Liu Y J and Zhang B C 2003 Improved remote sense monitoring on snow cover of china in winter *Journal of Applied meteorological science* **15**(Suppl.) pp 75-84
- [3] Wang J, Chen Z D, Li W J, Tan H, Lu A X and Li S 2000 Research on spectral reflectance properties of snow using moderate resolution imaging spectroradiometer data *Journal of Glaciology and Geocryology* **22**(2) pp 165-70
- [4] Hao X H, Wang J, and Li H Y 2008 Evaluation of the NDSI threshold value in mapping snow cover of MODIS-a case study of snow in the middle qilian mountains *Journal of Glaciology and Geocryology* **30**(1) pp 132-38
- [5] Nolin A W 2010 Recent advances in remote sensing of seasonal snow *J. Glaciol.* **56** pp 1141-50



- [6] Bergeron T 1965 On the low-level redistribution of atmospheric water caused by orography *International Conference on Cloud Physics* Tokyo
- [7] Choulaton T W and Perry S J 1986 A model of the orographic enhancement of snowfall by the seeder-feeder mechanism *Q. J. R. Meteorol. Soc.* **112** pp 335–45
- [8] Zängl G 2008 The temperature dependence of small-scale orographic precipitation enhancement *Q. J. R. Meteorol. Soc.* **134** pp 1167–81.
- [9] Stoelinga M T, Stewart R E, Thompson G and Theriault J M 2013 Microphysical processes within winter orographic cloud and precipitation systems *Mountain Weather Research and Forecasting* pp 345–408
- [10] Houze R A 2012 Orographic effects on precipitating clouds *Rev. Geophys.* **50** RG1001
- [11] Colle B 2004 Sensitivity of orographic precipitation to changing ambient conditions and terrain geometries: An idealized modeling perspective *J. Atmos. Sci.* **61** pp 588–606
- [12] Dore A J and Choulaton T W 1992 Orographic enhancement of snowfall *Environ. Pollut.* **75** pp 175–79
- [13] Lehning M, Löwe H, Ryser M and Raderschall N 2008 Inhomogeneous precipitation distribution and snow transport in steep terrain *Water Resour. Res.* **44** W07404
- [14] Xue M, Droegemeier K K and Wong V 2000 The advanced regional prediction system (ARPS)-A multiscale nonhydrostatic atmospheric simulation and prediction model. Part I: model dynamics and verification *Meteorol. Atmos. Phys.* **75** pp 161–93
- [15] Xue M, Droegemeier K K, Wong V, Shapiro A, Brewster K, Carr F, Weber D, Liu Y and Wang D 2001 The Advanced regional prediction system (ARPS)-A multi-scale nonhydrostatic atmospheric simulation and prediction tool. Part II: model physics and applications. *Meteorol Atmos. Phys.* **76** pp 143–65
- [16] Yamamoto Y, Potthoff M, Tanaka T, Kajishima T and Tsuji Y 2001 Large-eddy simulation of turbulent gas-particle flow in a vertical channel: effect of considering inter-particle collisions *Journal of Fluid Mechanics* **442** pp 303-34
- [17] Clift R 1978 *Bubbles, Drops and Particles* (New York: Academic)
- [18] Anderson R S and Haff P K 1988 Simulation of eolian saltation *Science* **241** pp 820–23
- [19] Shao Y and Li A 1999 Numerical modelling of saltation in the atmospheric surface layer *Bound-Lay. Meteorol.* **91** pp 199–225
- [20] Lopes A M G, Oliveira L A, Ferreira A D and Pinto J P 2012 Numerical simulation of sand dune erosion *Environmental Fluid Mechanics* **13**(2) pp 145-68
- [21] Raderschall N, Lehning M and Schar C 2008 Fine-scale modeling of the boundary layer wind field over steep topography *Water Resources Research* **44** W09425